The effect of noise barriers on viaducts on pollutant dispersion in complex street canyons

Tingzhen Ming [a], Fangyan He [a], Yongjia Wu [a,*], Tianhao Shi [a], Changrong Su [a], Caixia Wang [a], Zhengtong Li [b], Wei Chen [a], Renaud de Richter [c]

[a] *School of Civil Engineering and Architecture, Wuhan University of Technology, Wuhan 430070, China*
[b] *Department of Aeronautical and Aviation Engineering, The Hong Kong Polytechnic University, Hong Kong, China*
[c] *Tour-Solaire.Fr, 8 Impasse des Papillons, Montpellier F34090, France*

ARTICLE INFO

ABSTRACT

The noise reduction effect of noise barriers has been extensively studied, but the effect on pollutant dispersion remains unclear. A computational fluid dynamics (CFD) simulation is conducted to investigate the effects of different heights, lengths, and types of noise barriers and different wind speeds on pollutant dispersion in street canyons with viaducts. The field synergy theory of the convective mass transfer process is used for quantitative analysis of pollutant dispersion in street canyons. The results show that as the height and length of the noise barrier increase, the pollutant dispersion capacity decreases. As the wind speed increases, the rate of decrease in the average CO concentration declines. The effect of the wind speed on the synergistic improvement of the speed and concentration gradient vectors differs for different types of noise barriers. The performance follows the order: fully-closed noise barrier > left noise barrier > right noise barrier > semi-closed noise barrier. The different noise barrier types significantly impact the flow field and pollutant dispersion and reduce the CO concentration to varying degrees, except for the fully-closed type. The average CO concentration in the pedestrian breathing zone is reduced by a maximum of 55.85% on the leeward side and by 53% on the windward side, indicating that an appropriate noise barrier on the viaduct reduces noise pollution and improves the air quality in street canyons, especially in the pedestrian breathing zone.

1. Introduction

Urbanization has increased population and traffic densities, worsening urban ventilation. Motor vehicles are necessary for travel. Their surge in numbers and the resulting traffic congestion contribute significantly to particulate and gaseous pollutants in urban areas, and the resulting traffic noise pollution cannot be underestimated. It was found that approximately 50% of the adult mortality from air pollution or 22,000 deaths per year could be attributed to traffic sources in Austria, France, and Switzerland [1]. They estimated that traffic was responsible for an additional 15,000 cardiovascular hospital admissions in these three countries annually. Therefore, it is critical to analyze the dispersion characteristics of traffic-generated pollutants in urban areas to improve environmental quality.

Nicholson [2] first introduced the concept of the street canyon in 1975 and defined it as a street surrounded by buildings on both sides, resulting in a canyon. Subsequently, researchers investigated the street canyon microenvironment since it represents a major area for human activities. Numerous computational fluid dynamics (CFD) simulations

and water/wind tunnel experiments and field measurements [3–6] have been carried out to study the impacts of different urban designs on urban airflow and pollutant dispersion [7,8]. Various factors influencing urban pollutant dispersion have been examined, including the geometry of street canyons [9–12], building geometry [13,14], local atmospheric conditions [15–18], chemical reactions of pollutants [17–20], thermal effects caused by solar radiation [14,21], turbulent kinetic energy caused by vehicle movement [22–25], obstacles of street canyon facilities such as tree plantings [3,26], and viaducts [27,28]. For example, high wind speed and an oblique wind direction are favorable conditions, whereas a perpendicular wind direction increases the pollutant level. In an asymmetric street canyon, one vortex occurred in a step-up street canyon, while two counter-rotating vortices were observed in the step-down street canyon. Step-up street canyons and street canyons with non-uniform building heights are beneficial to pollutant dispersion. The chemical reactions of pollutants depend on the layout of street canyons, atmospheric conditions and the presence of other chemicals. The height of a viaduct should be lower than the top of the street canyon to prevent a lid effect. Heating on the windward side or unsf thermal stratification provide favorable conditions and improve air quality in street canyons. The wind direction had a significant influence on the turbulent kinetic energy induced by moving vehicles. In addition, planting low foliated
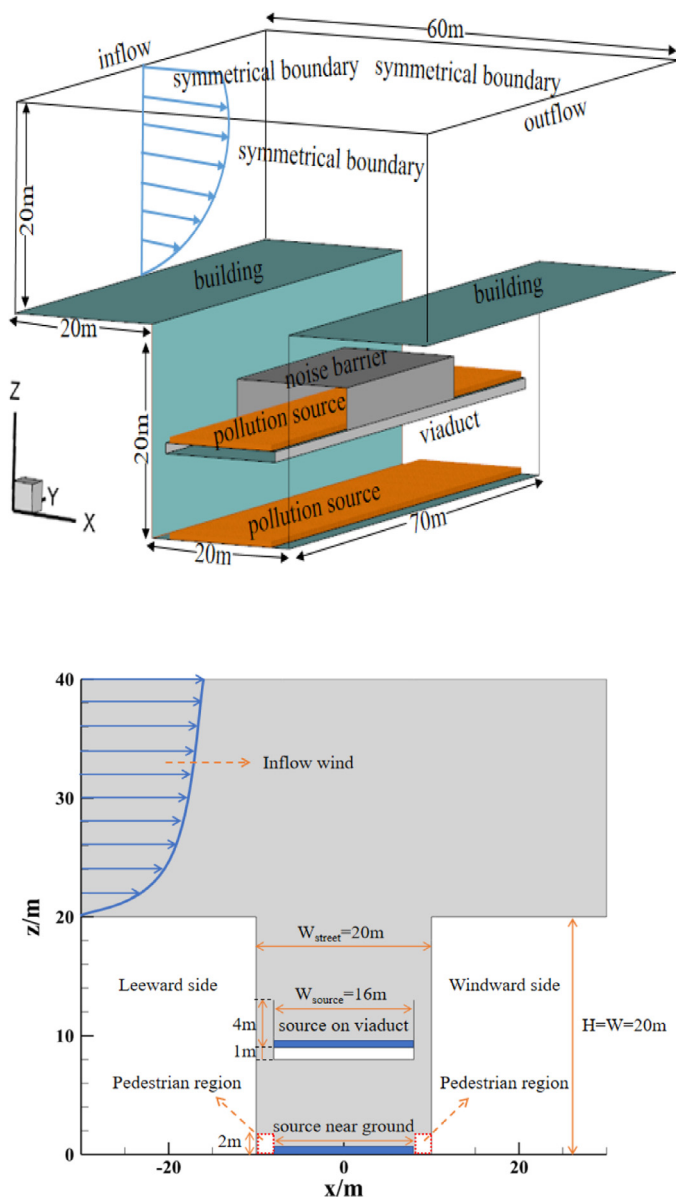

Fig. 1. Geometric model and details of street canyons.

trees and aligning them nonuniformly in the canyon improve air quality. Although viaducts in street canyons can alleviate local traffic congestion in urban areas, their lid effect worsens the air quality in street canyons. Increasing urbanization has led to greater building heights on both sides of urban roads [29,30], further aggravating environmental pollution in street canyons. Moreover, traffic noise pollution adversely affects human health [7,31]. Noise effects include annoyance [32], deterioration of sleep quality [33], and increased risk of cardiovascular diseases [34], diabetes [35], and metabolic disorders [36].

Quite a few researches including field studies [37–40], numerical simulations [41–44], and wind tunnel measurements [45,46] have been reported to investigated the impacts of road-side noise barriers on near-road air quality. Recently, the urban traffic pressure has increased rapidly with the continuous deepening of Chinese urbanization process, complex three-dimensional traffic systems consisting of one or more of the viaducts, underground tunnels, turntables, etc. are constantly updating the traditional and simple urban traffic systems. The frequently moving vehicles in the three-dimensional traffic system cause very serious noise pollution to the residents and pedestrians of the surrounding buildings. Setting noise barriers on the viaducts become an effectively

way to reduce traffic noise but affects the pollutant dispersion characteristics in street canyons. However, there is a lack of comprehensive studies on the impacts of noise barriers on viaducts on air quality. Noise barriers can also reduce indoor noise pollution, and it was investigated the impact of the viaduct configuration on gaseous and particle dispersion. The results showed that noise barriers on the viaduct slowed down the flow above it and slightly increased indoor concentrations of gaseous pollutants and the number of indoor particulates due to the enhanced particle deposition onto viaduct surfaces [47]. They enhance the vertical dispersion and initial mixing of pollutants and create a recirculation zone behind the barrier, transporting emissions from the highway towards the wall and reducing near-road pollutant concentrations [45]. Li et al. [48] studied the impacts of noise barriers on near-viaduct air quality in Xi'an, China. The results suggested beneficial effects of noise barriers and combination barriers for mitigating the air pollution near viaducts. It was investigated that the effects of different shapes of noise barriers on automobile emission reduction. An optimized range of the T-shaped noise barrier was the best choice [49]. He et al. [50] explored the impact of the street aspect ratio and the presence of viaducts and noise barriers on the flow and vehicular passive pollutant exposure in full-scale street canyons (H/W=1-6, W=24 m), suggesting that road barriers slightly increased pollutant exposure in near-road buildings with H/W=1 and slightly reduced them in buildings with H/W=3 and 5. Hang et al. [47] examined the impact of a viaduct on the personal intake fraction and found that the viaduct and noise barrier substantially affected the vortex center and pollutant dispersion mode; the location of the pollution source was a major contributor to pollutant dispersion. Zhi et al. [43] found that noise barriers on viaducts affected the flow field in street canyons. Two main vortices and two or three secondary vortices were generated in the street canyon with a viaduct and noise barrier, but only one main vortex was observed without a viaduct and noise barrier. Hao et al. [42] investigated the effects of viaducts and noise barriers on the flow pattern and particulate matter dispersion in street canyons. The results demonstrated that viaducts were associated with more sources of particulates and significantly affected flow patterns. The effect of a noise barrier on the vortex and pollutant distribution depends on local conditions.

From the literature review shown above, we can see that some scholars have carried out very interesting investigation on the pollutant dispersion characteristics in the street canyon-viaduct system by setting noise barriers and found that noise barriers have remarkable impacts on the diffusion of vehicle pollutants. However, there is still a lack of reliable theory and methodology to guide how to design the types of noise barriers and enhance pollutant dispersion in complex urban street canyons. Based on this, the field synergy theory is first introduced to quantitatively assess the pollutant dispersion in street canyon-viaduct system with various noise barriers by comparing with the cases of different types, heights, and lengths of noise barriers and different ambient wind speeds. The analysis result is helpful for the guidance of the complex transportation system planning and air quality improvement in urban areas.

2. Methodology

2.1. Physical model

We establish an ideal urban isolated street canyon model, as shown in Fig. 1. The height of the building (20 m in the Z-axis direction) is equal to the width of the street (in the X-axis direction), i.e., the aspect ratio of the street canyon model (building height/street width= H/W) is 1. The street length (in the Y-axis direction) is 70 m. At the center of the canyon is a two-way four-lane street, with a lane width of 4 m wide and a total width of 16 m, which is the same as the situation on viaduct. Sidewalks with a width of 2 m are located on both sides of the street. The inlet and outflow boundaries are 20 m from the upstream and downstream buildings. The upper boundary is 40 m from the ground.
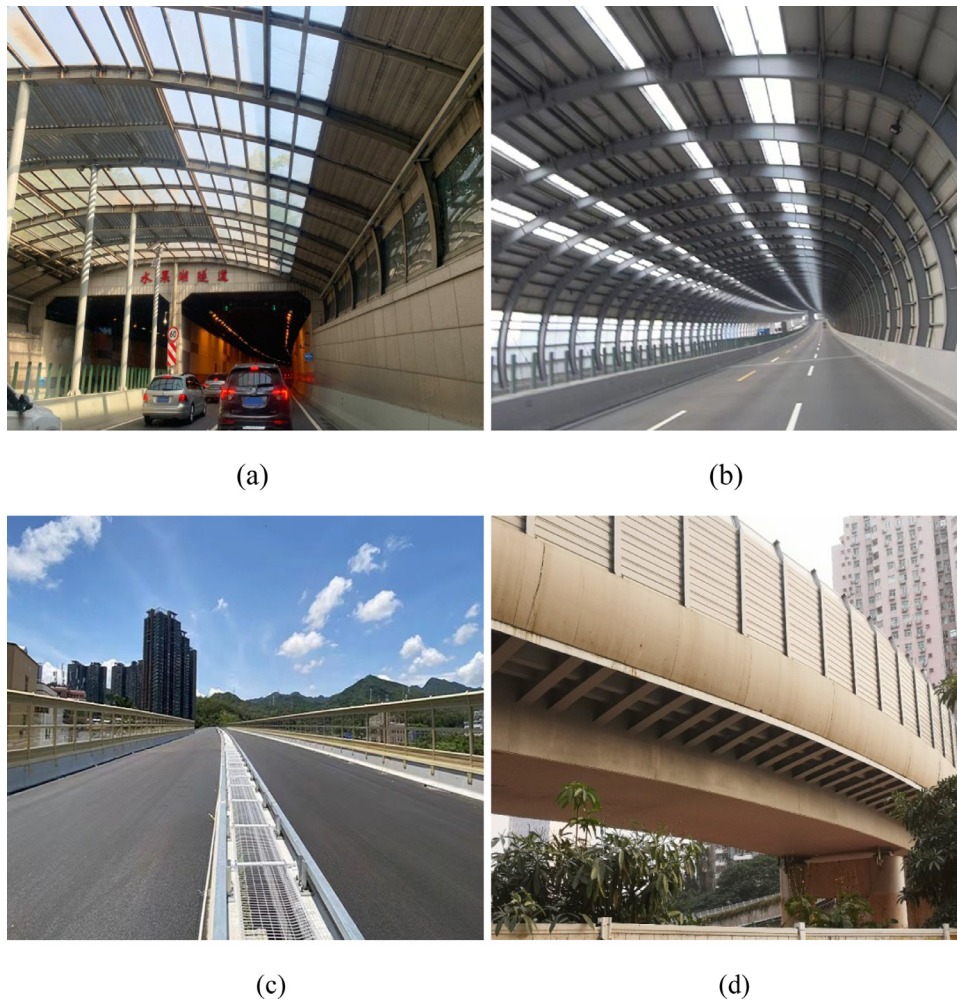
(a)

(b)

(c)

(d)

Fig. 2. Different types of noise barrier in real life: (a, b) fully-closed; (c) semi-closed; (d)single-sided.

The height of the viaduct is 0.4 H = 8 m, the height of the noise barrier is 4 m, the length of the noise barrier is 30 m, and the length of each side is 20 m. A uniform volumetric pollutant source is located on the ground and above the viaduct, with an emission intensity of 10^{-7} kg/(m^3.s). The length is equal to that of the street, and the height is 0.5 m. Moreover, The model in Fig. 1 is a simplified fully-closed noise barrier, while the conventional types of noise barriers include fully-closed noise barrier, semi-closed noise barrier, and single-sided noise barrier (left-sided or right-sided),as shown in Fig. 2.

2.2. Mathematical model

The renormalization group (RNG) k-ε turbulence model is a modification of the standard k-ε model. Several studies have used it to simulate urban airflow fields and pollutant dispersion, producing reliable validation results [51,52]. The continuity equation, momentum equation, pollutant transport equation, and the RNG k-ε equation are defined as follows:

Continuity equation:

$$\frac{\partial U_i}{\partial x_i} = 0 \tag{1}$$

Conservation of momentum equation:

$$\frac{\partial U_i}{\partial t} + U_i \frac{\partial U_j}{\partial x_j} = -\frac{1}{\rho}\frac{\partial p}{\partial x_i} + \frac{\partial}{\partial x_j}\left(v\frac{\partial U_i}{\partial x_j} + \frac{\partial U_j}{\partial x_i} - \overline{u_i' u_j'}\right) + \left(\frac{\rho - \rho_0}{\rho_0}\right)g_i \tag{2}$$

Turbulent kinetic energy equation k:

$$\frac{\partial k}{\partial t} + U_j\frac{\partial k}{\partial x_j} = \frac{\partial}{\partial x_j}\left[\left(v + \frac{v_t}{\sigma_k}\right)\frac{\partial k}{\partial x_j}\right] + G - \varepsilon \tag{3}$$
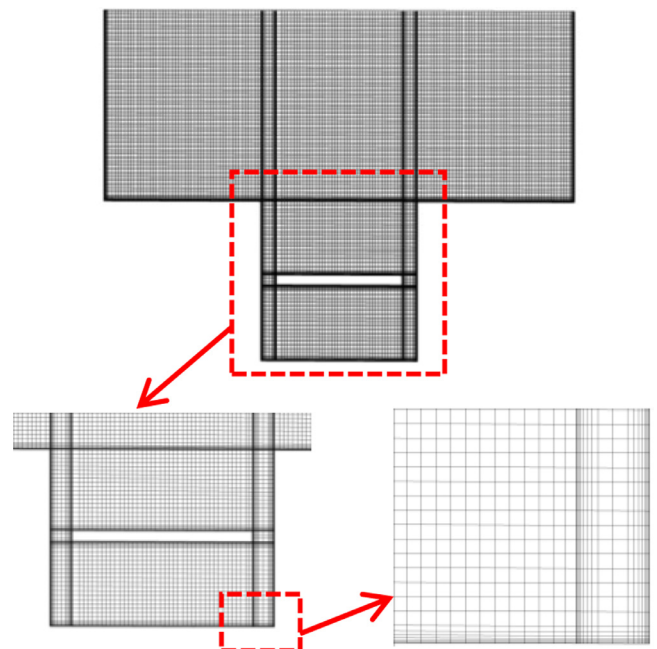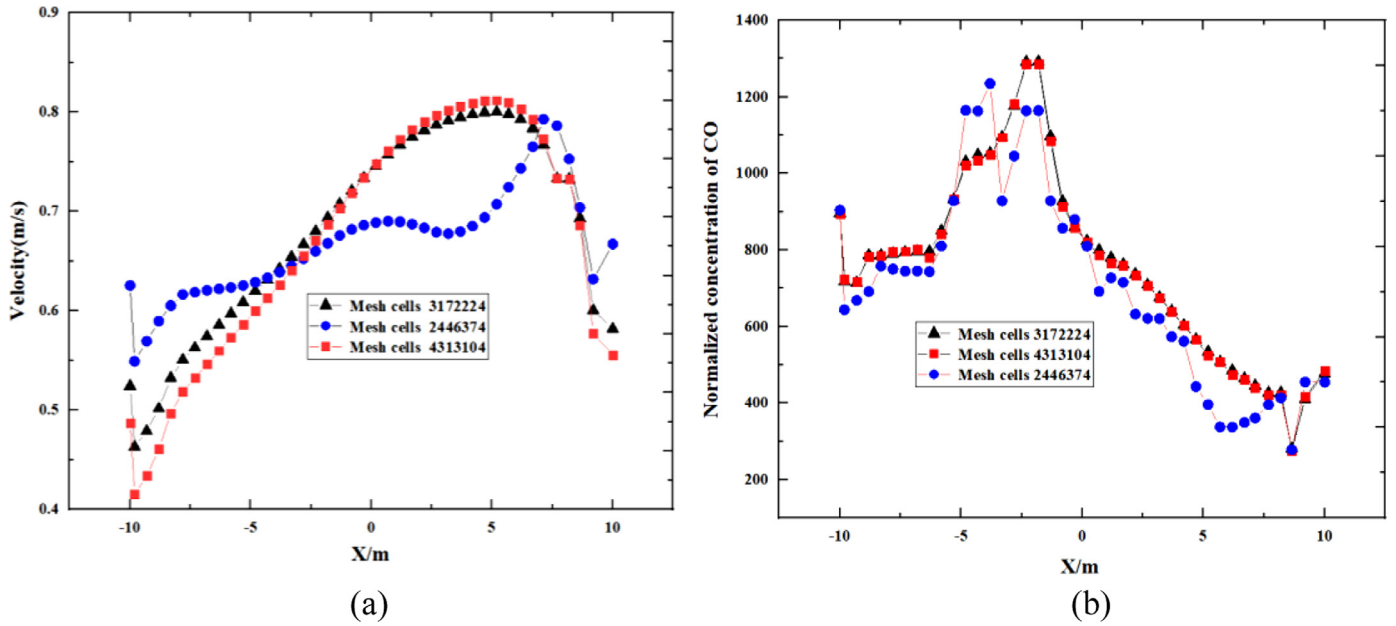

Fig. 3. Schematic diagram of the mesh.

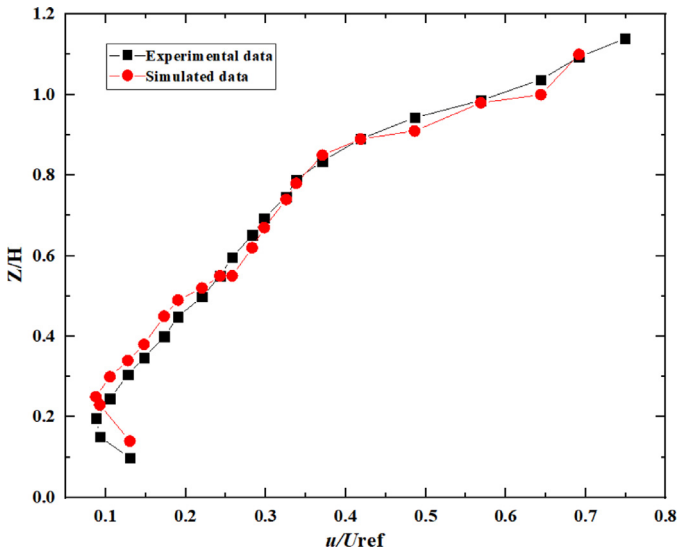**Fig. 4.** (a) Wind velocity and (b) normalized concentration of CO on the Y = 0 m line for different mesh sizes.

Fig. 5. Comparison of normalized velocity obtained from the simulation and experiments.

Fig. 6. Comparison of normalized concentration obtained from the simulation and experiments.

Dissipation rate of turbulent kinetic energy ε:

$$\frac{\partial \varepsilon}{\partial t} + U_i \frac{\partial \varepsilon}{\partial x_i} = \frac{\partial}{\partial x_j}\left[\left(\nu + \frac{\nu_t}{\sigma_\varepsilon}\right)\frac{\partial \varepsilon}{\partial x_j}\right] + C_{1\varepsilon}\frac{\varepsilon}{k}G - \left[C_{2\varepsilon} + \frac{C_\mu \rho \eta^3 \left(1 - \frac{\eta}{\eta_0}\right)}{1 + \beta\eta^3}\right]\frac{\varepsilon^2}{k} \tag{4}$$

where υt is the turbulent viscosity coefficient; $\eta = 0.5(k/\varepsilon)(G/\nu_t)$; $C\mu$, $C_{1\varepsilon}$, $C_{2\varepsilon}$, β, and η_0 are constants (0.09, 1.44, 1.92, 0.012, and 4.38, respectively). σ_k and σ_ε are the Prandtl numbers (1.0 and 1.3, respectively); $\eta = 0.5 (k/\varepsilon)(G/\nu_t)$.

Component transport equation:

$$\frac{\partial C_i}{\partial t} + U_j \frac{\partial C_i}{\partial x_j} = \frac{1}{\rho}\frac{\partial}{\partial x_j}\left[\left(D_i + \frac{\mu_t}{Sc_t}\right)\frac{\partial C_i}{\partial x_j}\right] + Sc \tag{5}$$
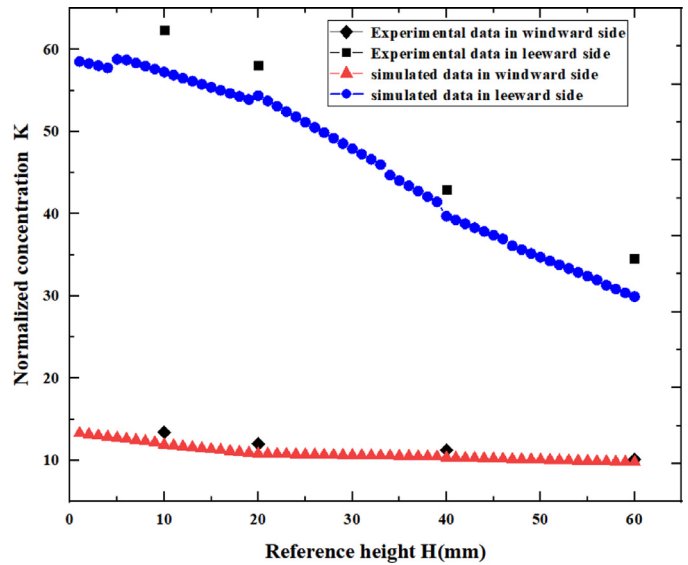
where C_i is the species concentration; C is the species volume; D_i is the diffusivity coefficient; S_c represents the pollutant source term defined in this study, which is $10^{-7}\text{kg}/(\text{m}^3 \cdot \text{s})$.

2.3. Boundary conditions

The gradient wind is the velocity inlet boundary and is perpendicular to the street canyon. The outlet boundary is set to a free-flow condition. The upper boundary and sides of the computing domain are set as symmetrical boundary conditions (zero-gradient boundary). Turbulence does not fully develop in the near-wall area and near-ground area of the building. A standard wall function is used for near-wall correction on the wall, viaduct, noise barrier, and bottom of the building. All the other wall surfaces have slip wall boundary conditions. The vertical characteristics of the ambient wind are affected by the terrain, especially the roughness. Therefore, the gradient wind is used to represent
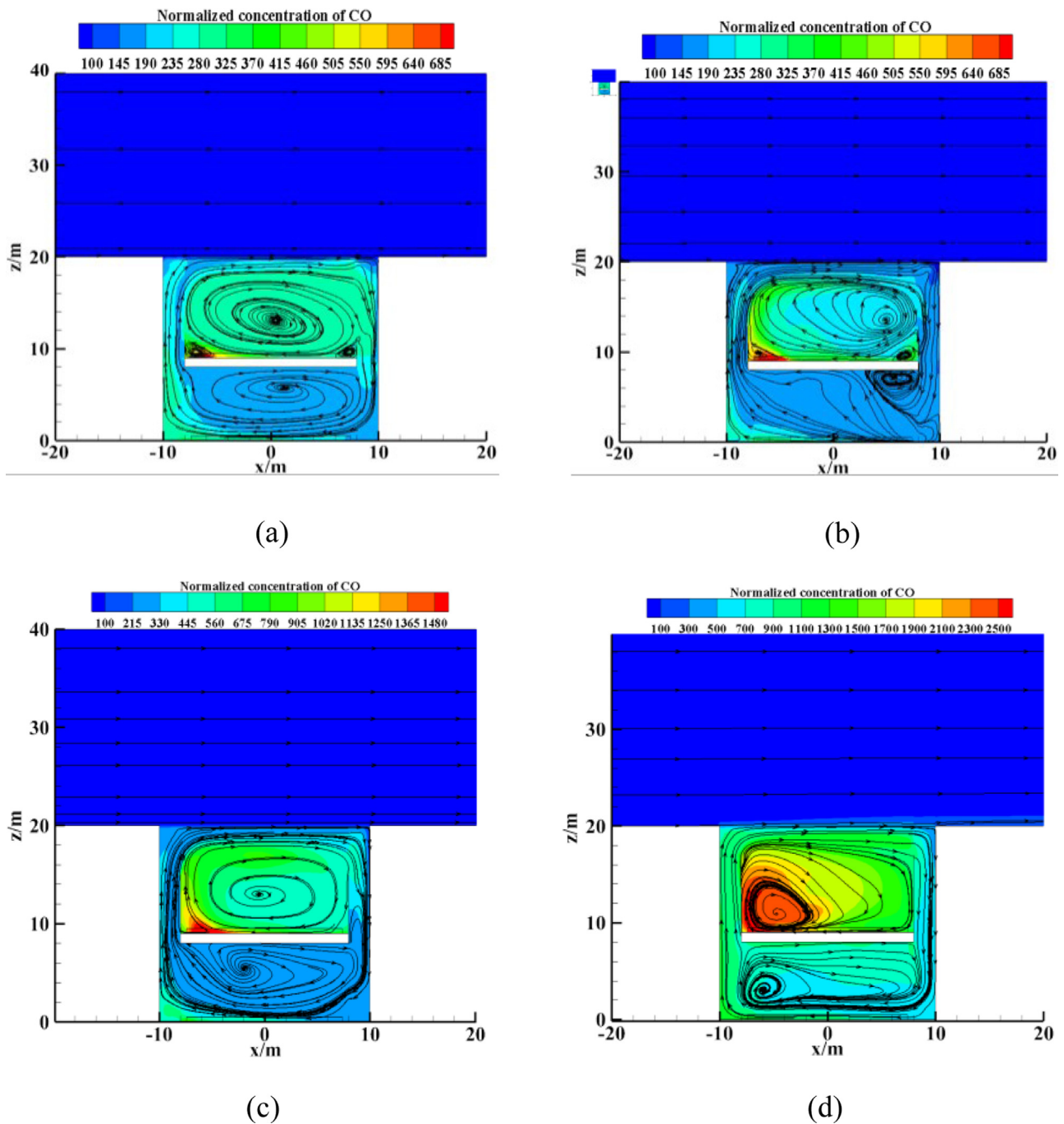
Fig. 7. Contours of the flow field and normalized CO concentration at y=0 for noise barriers with different heights: (a) 2 m; (b) 4 m; (c) 6 m; (d) 8 m.

the ambient wind speed. The wind speed for the inlet boundary condition follows an exponential or logarithmic law [53,54]. In this study, a user-defined function is used to define the exponential growth of the velocity at the inlet. The turbulent kinetic energy and turbulent dissipation rate are defined as follows:

$$U_z = U_{ref} \left(\frac{z - 20}{z_{ref}} \right)^a \qquad (6)$$

$$k = \frac{(U^*)^2}{\sqrt{C_\mu}} \qquad (7)$$

$$\varepsilon = \frac{U_*^3}{\kappa z} \qquad (8)$$

where U_{ref} represents the velocity at the reference height ($z_{ref} = 20$ m). α is the ground roughness index (0.2). U^* represents the friction velocity. κ represents the von Karman constant (0.42); $C\mu$=0.99 represents the empirical constant. We considered four incoming wind speeds ($U_{ref} = 2$ m/s, 4 m/s, 6 m/s, and 8 m/s) to represent very low, low, medium, and high wind speeds, respectively. The lowest wind speed ($U_{ref} = 2$ m/s) corresponds to the smallest Reynolds number ($Re= U_{ref}$ H/v=3002550) so that all simulations meet the Reynolds number independence (Re>11000).

2.4. Mesh generation and sensitivity analysis

Discretization of the computing domain is an essential component of numerical simulations. The advantages of structured grids are that
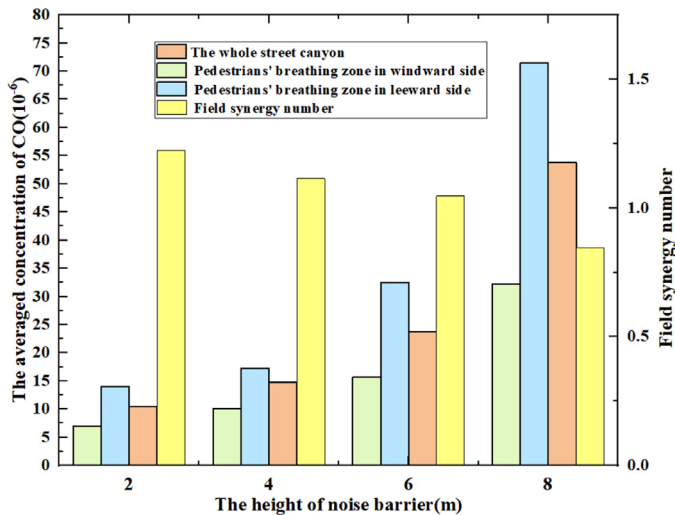
Fig. 8. Histogram of field synergy number and average CO concentration.

the mesh structure is simple, regular, and convenient, the calculation is easy, and the memory requirement is low. Because the geometric model in this study is relatively simple and regular, we use a structured grid to ensure high calculation accuracy and low computational complexity. Eight layers of boundary grids are used for the building walls, the ground, the viaduct, and the noise barrier to ensure the applicability of the standard wall function. The first layer mesh is 0.02 m to ensure that the y+ at the boundary is 20. The internal mesh layout is $\Delta x \times \Delta y = 0.4 \times 0.4$, and the mesh is coarse in the boundary area of the computational domain. The schematic diagram of the mesh is shown in Fig. 3.

The commercial CFD software ANSYS FLUENT 19.2 is used for numerical simulation. The incoming wind is compiled by the user-defined function (UDF). The second-order upwind type is used for the discretization of the convection term. The Green-Gaussian node method is used for gradient interpolation. The experimental calculation method uses the SIMPLE algorithm, and the standard algorithm is used for the pressure interpolation. The RNG k-ε model is used. The convergence factor of the energy equation is 1×10^{-8}, and the convergence factor of the other variables is 1×10^{-5}.

We verified the mesh independence using three grid sizes (2446374, 3172224, and 4313104) and the same computer and same working conditions (U_{ref} = 2 m/s). Fig. 3 shows the grid independence test results for the centerline of the street in the X-axis direction (Y = 0 m, Z = 2 m, X from -10 m to 10). The velocity and the normalized CO concentration on this line for the three grid sizes are shown in Fig. 4(a) and (b), respectively. The results are similar for the 3172224 and 4313104 grid sizes, and the maximum error of the speed and the normalized CO concentration is less than 5%. The error is the largest for the 2446374grid size. A further increase in the grid size from 3172224 to 4313104 does not change the speed and pollutant concentration substantially, demonstrating the accuracy of the numerical solution and the grid independence. Therefore, we used a grid size of 3172224.

2.5. Pollution source

Pollutants in urban streets include gaseous pollutants and solid particles. The dispersion of the particles is affected by wind speed, particle size, thermal buoyancy, air humidity, and other factors. CO is a colorless and odorless gas but is highly toxic; CO poisoning is the most common type of fatal poisoning in many countries [55]. Furthermore, the proportion of CO in vehicle exhaust is relatively large, and its chemical properties are relatively stable; thus, CO does not readily react with other substances in the air. We used CO as a tracer pollutant to simplify the

analysis and investigate its diffusion in urban street canyons. In order to effectively evade the effect of factors such as the height of buildings on both sides, street geometry and other factors on the calculation results, the pollutant concentrations were normalized to obtain a standardized concentration as follows:

$$K = \frac{\rho_{co} \, C U_{ref} \, LH}{S_c V_c} \tag{9}$$

where C represents the pollutant concentration (CO mass fraction) obtained from the FLUENT simulation results; U_{ref} (m/s) represents the wind speed at the reference height z_{ref}; ρ_{co} is the density of CO (=1.295 kg/m^3); L (m) is the length of the pollution source; H (m) is the height of the building; S_c is the total emission intensity of the pollution source (kg/(m^3•s)); V_c (m^3) is the control volume of the pollution source.

2.6. Field synergy theory

Pollutant dispersion in urban street canyons is a convective mass transfer driven by the ambient wind [56].Ming et al. [57] applied the field synergy theory to the study of pollutant dispersion in street canyons. Results show that adding wind catchers can greatly improve the air quality of the step-down street canyon and reduce the average pollutant concentrations in the street canyon by 75%. Different types of noise barriers in street canyons have different impacts on pollutant dispersion. The Reynolds number Re and Schmidt number Sc remain unchanged due to the same physical properties of the wind. The field synergy number Fc_m can be used to evaluate the effect of convective mass transfer. The greater the field synergy number Fc_m, the better the synergy effect of the velocity field and the concentration field is, and the stronger the convective mass transfer effect is. The field synergy number is expressed as follows:

$$Fc_m = \frac{\int_\Omega \bar{U} \cdot \overline{\nabla C} dV}{V} \tag{10}$$

The Sherwood number is the ratio of the boundary diffusion resistance of the fluid to the convective mass transfer resistance, characterizing the relative size of the convective mass transfer and diffusion mass transfer. Because the pollutant dispersion in street canyons is driven by the ambient wind, the convective mass transfer process dominates. Therefore, the physical properties differ for different wind speeds. The Sherwood number can be used to measure the strength of the pollutant diffusion effect in the street canyon. The larger the Sherwood number Sh, the higher the synergy between the velocity field and the concentration field is, and the stronger the convective mass transfer effect is. Eq. (11) shows that the Sherwood number depends on the Reynolds number, the Schmidt number, the synergy angle of the velocity vector, and the concentration gradient vector, i.e., the value of the dot product of the two vectors in the target area. The Sherwood number is expressed as follows:

$$Sh = Re S_c \frac{\int_\Omega \bar{U} \cdot \overline{\nabla C} dV}{V} \tag{11}$$

3. Results and discussion

3.1. Validation study

We used the wind tunnel experimental data to evaluate the reliability of the street canyon model with an aspect ratio of 1 [58]. The size of the wind tunnel was 10 m × 0.3 m × 0.5 m. Ten rectangular parallel pipes (0.298 m × 0.1 m × 0.1 m) of the same size were arranged at the tuyere, and they were placed at an equal interval of 0.1 m (H) to simulate multiple street canyons. We used the fifth street canyon as the target street canyon. The LDA system, a fiber-optic system (model 55X, supplied by Dantec Dynamics), automatically controlled and measured the change in wind speed in the z-axis direction at y/H=0, x/H=0.75 in the target street canyon. Based on this wind tunnel experiment, an identical
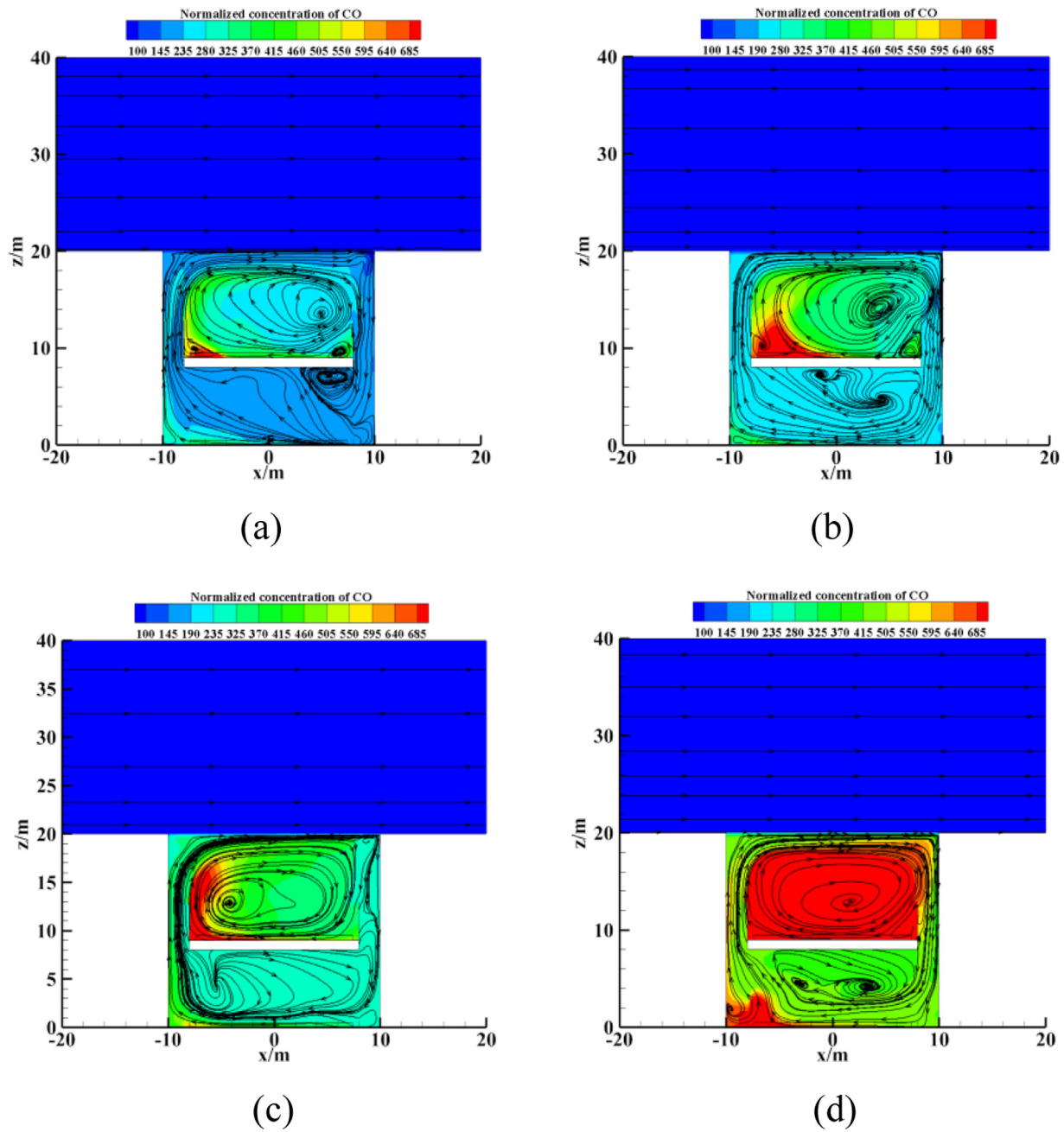
Fig. 9. Contours of the flow field and normalized CO concentration at y=0 for noise barriers with different lengths: (a) 30 m; (b) 40 m; (c) 50 m; (d) 60 m.

geometric model was established, and consistent boundary conditions were set. The calculation result is shown in Fig. 5. The data obtained from the numerical simulation agrees well with the wind tunnel test data. Although there is a slight deviation, the overall error is within the acceptable range. The results indicate that the proposed model and the numerical simulation method can be used to analyze the atmospheric field in the street canyon.

The reliability of simulating the pollutant concentration and dispersion in urban street canyons is verified using the wind tunnel experimental data obtained from Meroney et al. [59]. According to the wind tunnel experiment, a model of an ideal street canyon with an aspect ratio of 1 (H/B=1, H=0.06 m) is established. The building height is 0.06 m, and the pollutant discharge is linear on the ground parallel to the y-axis. The tracer gas is ethane, the line source length is 0.90 m, and the dimensionless concentration K (ethane) is obtained by the dimension-

less U_{ref} (free flow wind speed, 1 m/s) at 0.65 m above the street. The ethane mixture emission volume is Qe=1.4 l/h, and the air emission volume is Qa=100 l/h. The numerical simulation results are shown in Fig. 6. The simulation results of the dimensionless concentration on the windward and leeward sides are compared with the wind tunnel experimental data. The trends are in good agreement, indicating that the established model and numerical simulation methods can be utilized to analyze the pollutant concentration field in the street canyon.

3.2. Effect of the noise barrier height

Fig. 7 shows the flow field and dimensionless CO concentration distribution at y=0 for noise barriers with different heights. Four semi-closed noise barriers with heights of 2 m, 4 m, 6 m, and 8 m were analyzed. As the noise barrier height increases, the flow field in the street canyon does not change substantially. It can be divided into two main
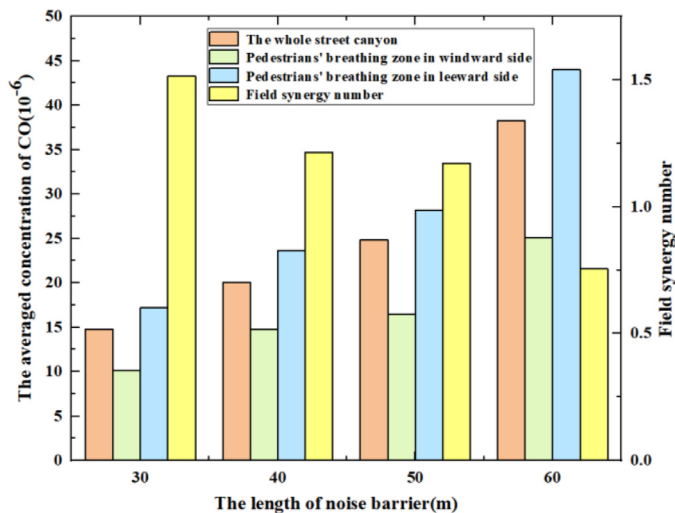
Fig. 10. Histogram of the field synergy number and average CO concentration.

vortices above and below the viaduct, and the center of the vortex exhibits a slight shift. Due to the vortex structure in the street canyon, the pollutants are concentrated near the ground on the leeward side of the street canyon and above the viaduct. As the height of the noise barrier increases, the level of pollutant dispersion decreases, and the average pollutant concentration in the street canyon increases.

Fig. 8 shows the CO concentration and field synergy number of noise barriers with different heights. As the height of the noise barrier increases from 2 m to 4 m, the increase in the concentration is less than 50% in the entire street canyon and in the pedestrian breathing area, and the field synergy number decreases by 8.92%. As the height of the noise barrier increases from 4 m to 6 m, the average pollutant concentration in the street canyon increases by 60.63%. The average concentration in the pedestrian breathing area increases by 88.62% on the leeward side and by 54.62% on the windward side. The field synergy number decreases by 6.23%. As the noise barrier height increases from 6 m to 8 m, the average pollutant concentration in the street canyon increases by 126.19%. The average concentration in the pedestrian breathing area increases by 120.23% on the leeward side and by 106.23% on the windward side, and the corresponding field synergy number is 19.31% lower. The results indicate that increasing the height of the noise barrier does not improve pollutant dispersion. The synergistic effect between the velocity field and the pollutant concentration field in the street canyon is weakened, the number of synergies decreases, and the pollutant concentration increases. A noise barrier with a height of 8 m prevents the outward diffusion of pollutants on the viaduct and substantially reduces the diffusion of pollutants below the viaduct because the noise barrier blocks the incoming wind. The high-concentration area above and below the viaduct increases significantly as the noise barrier height increases. The peak concentration above the viaduct of the 8-m high noise barrier is 4 times that of the 2 m high noise barrier, and the synergy number is about 30% lower.

3.3. Effect of the noise barrier length

Fig. 9 shows the flow field and dimensionless CO concentration distribution at y=0 for noise barriers of different lengths. Four semi-closed noise barriers with lengths of 30 m, 40 m, 50 m, and 60 m were analyzed. As the length of the noise barriers increases, the center of the main vortex on the viaduct shifts slightly, but there is always only one main vortex. The flow field is more complex below than above the viaduct. When the length of the noise barriers is 40 m and 60 m, two main vortices are formed below the viaduct. In contrast, only one main vortex occurs for the noise barriers with lengths of 20 m and 50 m. The noise

barrier restricts the flow, reducing the pollutant diffusion between the noise barriers on the viaduct and below the viaduct. Fig. 9(a–d) shows that the area of high CO concentration increases significantly with an increase in the noise barrier length. Due to the vortex structure in the street canyon, the pollutant is concentrated near the ground on the leeward side of the street canyon and above the viaduct.

Fig. 10 shows the comparison of the average CO concentration and field synergy number for noise barriers with different lengths. As the length of the noise barrier increases, the level of pollutant diffusion decreases, and the synergistic effect of the velocity field and the pollutant concentration field in the street canyon weakens. The average CO concentration in the pedestrian breathing area on the windward and leeward sides and in the entire street canyon show an upward trend. The field synergy number continues to decline. As the length of the noise barrier increases from 30 m to 60 m, the synergy number decreases by about 43%, the average CO concentration in the street canyon increases by 160%, and the CO concentration in the pedestrian breathing area increases by 155% on the leeward side and by 147% on the windward side. Thus, the environmental quality in the street canyon decreases with the increasing length of the barrier.

3.4. Effect of the noise barrier type

Fig. 11 shows the flow field and dimensionless CO concentration at y=0 for different types of noise barriers. The presence of viaducts and noise barriers in urban street canyons significantly changes the distribution of pollutants and flow fields in street canyons. Fig. 11(a–e) shows the noise barrier on the viaduct significantly affects the flow field distribution in the street canyon, especially below the viaduct. Without noise barriers on the viaduct, vortices occur on the viaduct and below the bridge. The incoming wind is deflected by the noise barrier, and the pollutants diffuse more evenly. The main vortex is observed above the viaduct when a semi-closed noise barrier is present. The center of the vortex under the viaduct has shifted to the upper right, and the pollutants are concentrated near the ground on the leeward side of the street canyon and above the viaduct. The noise barrier reduces the area of high CO concentration, especially near the ground on the leeward side below the viaduct. When the viaduct has a single noise barrier (left or right), a main vortex forms above the viaduct. The flow field structure below the bridge is more complicated; there are two secondary vortices, and the peak concentration in the street canyon has decreased. The blocking effect is weaker for the single noise barrier than the semi-closed noise barrier, and the pollutant dispersion is more even. The fully-closed noise barrier prevents upward or downward pollutant dispersion. However, the maximum dimensionless CO concentration on the leeward side of the viaduct is 4 times higher than without a noise barrier. The vortex structure in the street canyon also differs from that of the other noise barrier types. Three vortices are formed in the street canyon, two vortices occur above the viaduct, and one main vortex is observed below the viaduct.

Fig. 12 shows the average CO concentration and field synergy number for different types of noise barriers. The noise barrier type influences the pollutant diffusion in the street canyon. As the field synergy number decreases, the synergistic effect between the velocity vector and the concentration gradient vector in the street canyon weakens, and the level of pollutant dispersion decreases. The field synergy number is the smallest (best synergistic effect), and the pollutant dispersion capacity is the best without a noise barrier. In contrast, the pollutant dispersion capacity is the worst for the fully-closed noise barrier. The field synergy number is 21.25% lower, and the average CO concentration in the street canyon is 132.23% higher than without a noise barrier. However, the different noise barrier types (except for the fully-closed one) reduce the average CO concentration in the pedestrian breathing areas. The average CO concentration in the pedestrian breathing areas is reduced by a maximum of 55.85% on the leeward side and 53% on the windward side. This result shows that noise barriers on the viaduct reduce noise
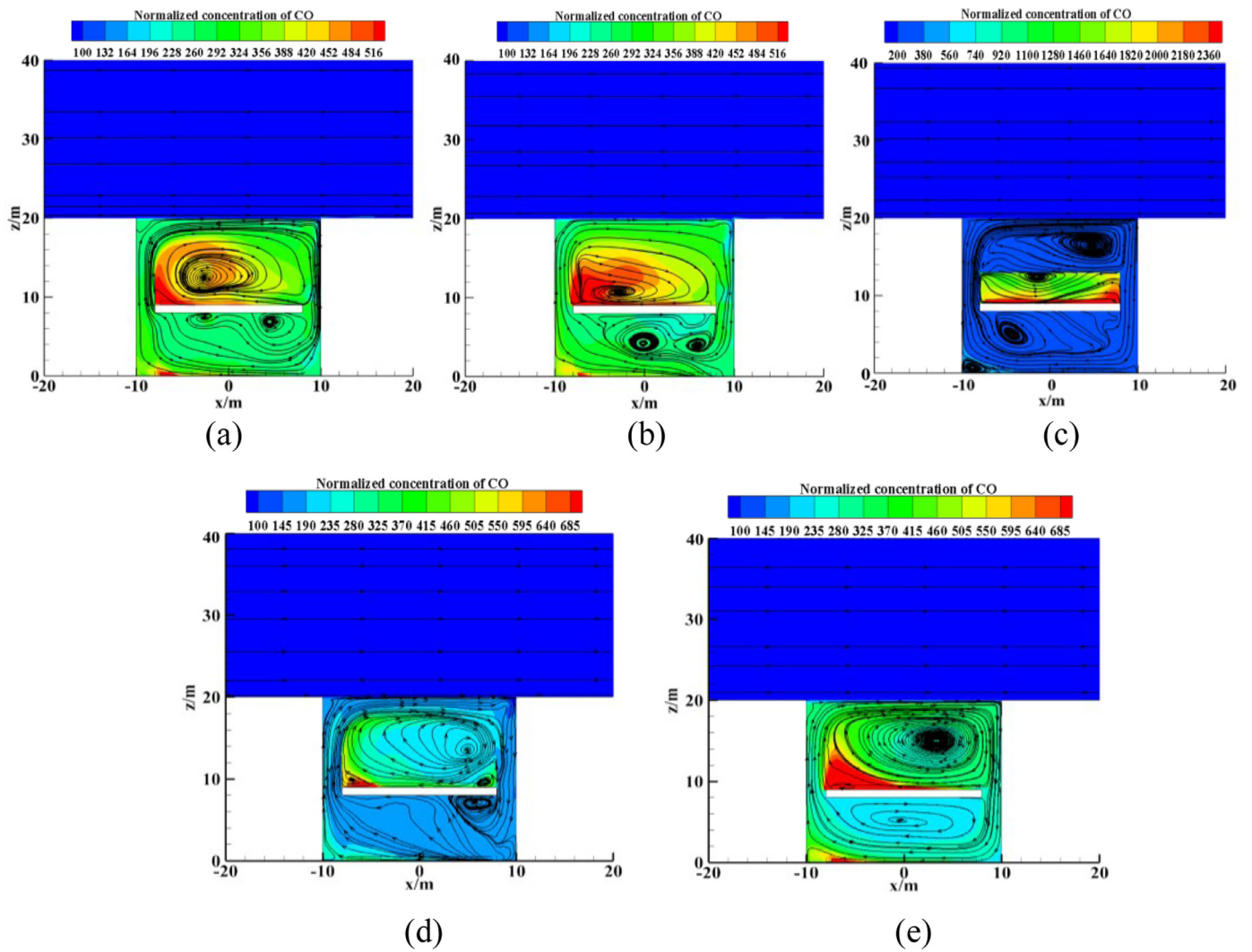
Fig. 11. Contours of the flow field and normalized CO concentration at y=0 for different types of noise barriers: (a) left noise barrier; (b) right noise barrier;(c) fully-closed noise barrier; (d) semi-closed noise barrier; (e) only viaduct without noise barrier.

and improve the air quality in densely populated areas, improving the health of residents and pedestrians.

3.5. Effect of wind speed on different types of noise barriers

Blocken et al. [60] found that the air quality in street canyons was lower when the ambient wind was vertical or parallel to the street canyon. We investigate conditions when the ambient wind is perpendicular to the street canyon and considered four inflow wind speeds (*Uref* =1 m/s, 2 m/s, 4 m/s, 8 m/s) to represent very low, low, medium, and high wind speeds. The wind speed and Reynolds number change with the wind speed. The field synergy number cannot be used to characterize the effect of convective mass transfer and pollutant diffusion. Thus, the Sherwood number is used to characterize the convective mass transfer and pollutant diffusion effects of different types of noise barriers at different wind speeds. The Sherwood number depends on the Reynolds number and field synergy number Eqs. (1)-(10) [57].

Fig. 13(a) shows the Sherwood number and the average CO concentration in the street canyon for different types of noise barriers and different wind speeds. The results indicate that the pollutant concentrations of all noise barrier types decrease as the wind speed increases. The Sherwood number of the single noise barrier (left or right) is the largest at an ambient wind speed of 2 m/s. The Sherwood number is the smallest for the fully-closed noise, indicating that the single noise bar-

rier has a structural advantage, with a more pronounced effect of the left noise barrier. As the wind speed increases, the pollutant diffusion of the different types of noise barriers improves to different degrees. The average CO concentration in the urban street canyons decreases with an increase in wind speed. The Sherwood number increases at different rates for the same increase rate of the wind speed, reflecting the different effects of the wind speed on the synergistic improvement of the speed and concentration gradient vectors of the different types of noise barriers. The performance follows the order fully-closed noise barrier > left noise barrier > right noise barrier > semi-closed noise barrier. As the wind speed increases from 2 m/s to 8 m/s, the Sherwood number of the fully-closed noise barrier increases the fastest, indicating that the wind speed has the largest influence on the fully-closed noise barrier.

Fig. 13(b) shows that the fully-closed noise barrier has the highest average CO concentration at a wind speed of 2 m/s. The concentration is about 3 times that of the single noise barrier. The reason is that the upward or downward pollutant diffusion on the viaduct is hindered by the fully-closed noise barrier. As the wind speed increases from 2 m/s to 6 m/s, the synergistic effect of the velocity and concentration gradient vectors is greatly enhanced, showing that the average CO concentration of the fully-closed noise barrier declines the fastest. However, the average CO concentration of this barrier is the biggest. The decline rate of the average CO concentration is similar for the single and semi-closed noise
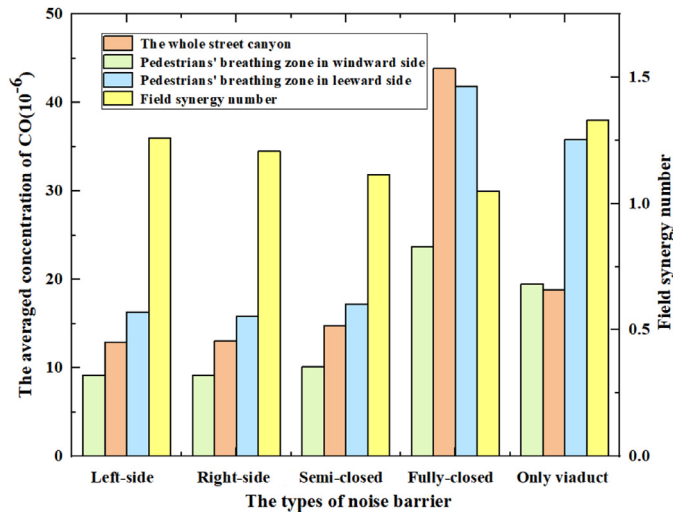
Fig. 12. Histogram of the field synergy number and average CO concentration.

barriers, and the former has the smallest average concentration. As the wind speed continues to increase from 6 m/s, the pollutant concentration does not change much. In addition, as the wind speed increases, the rate of decrease in the average CO concentration decreases, indicating that the influence of the wind speed on pollutant dispersion declines.

4. Conclusion

We investigated the effects of different heights, lengths, and types of noise barriers and different wind speeds on pollutant dispersion in complex street canyons with a viaduct. Computational fluid dynamics (CFD) was used to establish a model of the viaduct and noise barrier system in an urban street canyon. The pollutant dispersion in urban street canyons is a convective mass transfer process driven by the ambient wind. Our results provide reference data for urban planners to conduct quantitative evaluations of the air quality in human activity areas in street canyons. The field synergy theory of the convective mass transfer

process was used to analyze the pollutant dispersion capacity in a street canyon quantitatively. The conclusions are as follows:

(1) As the noise barrier height increased, the flow field in the street canyon did not change substantially. It was divided into two areas with vortices above and below the viaduct. The center of the vortex shifted slightly with an increase in the barrier height. Increasing the height did not improve pollutant dispersion. The synergistic effect between the velocity field and the pollutant concentration field in the street canyon weakened, the synergy number decreased, and the pollutant concentration increased. The highest pollutant concentration above and below the viaduct was observed at a noise barrier height of 8 m. The maximum CO concentration above the viaduct for the 8-m high noise barrier was 4 times that of the 2 m high noise barrier, and the synergy number was about 30% lower.

(2) As the noise barrier length increased, the center of the main vortex on the viaduct shifted slightly, but there was always only one main vortex. The flow field below the viaduct was more complicated. When the length of the noise barriers was 40 m and 60 m, two main vortices formed below the viaduct, whereas only one main vortex formed at barrier lengths of 20 m and 50 m. As the length of the noise barriers increased, the pollutant dispersion and the synergistic effect of the velocity field and the pollutant concentration field in the street canyon weakened. As the noise barrier length increased from 30 m to 60 m, the synergy number decreased by about 43%, the average CO concentration in the street canyon increased by about 160%, and the CO concentration in the key pedestrian breathing area increased by 155% on the leeward side and by 147% on the windward side, deteriorating the environmental quality in the street canyon and posing a threat to people's health.

(3) Noise barriers on viaducts in urban street canyons significantly changed the pollutant distribution and flow fields in the street canyon. The synergistic effect of the velocity vector and the concentration gradient vector was the strongest without a noise barrier, resulting in the highest pollutant diffusion capacity and the lowest average CO concentration. In contrast, the fully-closed noise barrier had the lowest pollutant diffusion performance and the highest average CO concentration. The average CO concentration in the street canyon was similar for the single and semi-closed barriers. However, in the densely populated pedestrian breathing areas, all noise barriers except the fully-closed one reduced the average CO concentrations to varying degrees. The averaged CO concentration was reduced by a maximum of 55.85% on the
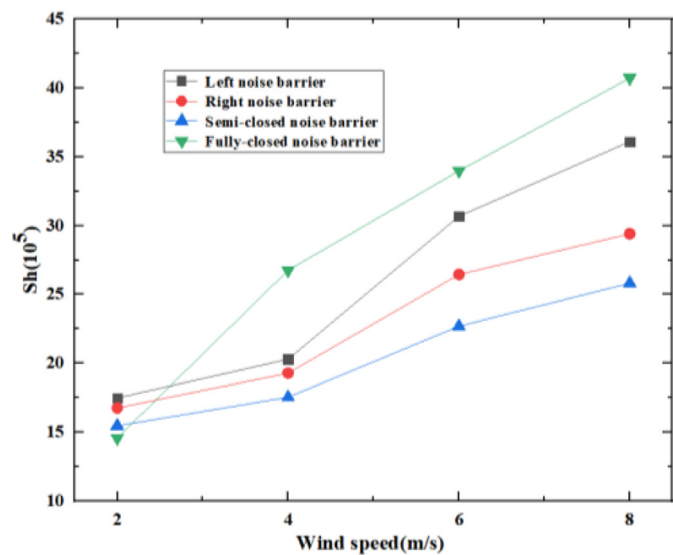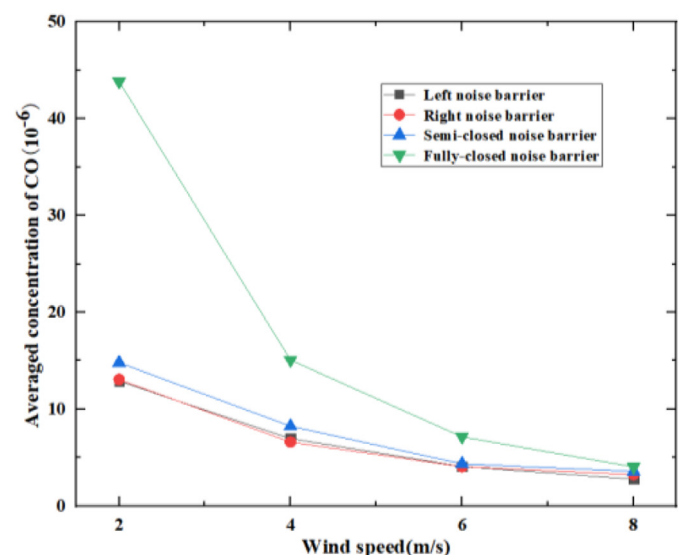
Fig. 13. Sherwood number and average CO concentration at different wind velocities for different types of noise barrier: (a) Sherwood number; (b) average CO concentration.

leeward side and by 53% on the windward side. The results showed that appropriate noise barriers on the viaduct reduced noise pollution and improved air quality in densely populated areas, benefiting the health of residents and pedestrians.

(4) As the wind speed increased, the rate of decline in the average CO concentration decreased, indicating a decreasing influence of the wind speed on pollutant dispersion. The Sherwood number increased at different rates for the same increase rate of the wind speed, reflecting the different effects of the wind speed on the synergistic improvement of the speed and concentration gradient vectors of different types of noise barriers. The performance followed the order fully-closed noise barrier > left noise barrier > right noise barrier > semi-closed noise barrier.

Conflict of Interest

None

Acknowledgements

References

[1] N. Künzli, R. Kaiser, S. Medina, M. Studnicka, O. Chanel, P. Filliger, M. Herry, F. Horak, V. Puybonnieux-Texier, P. Quénel, Public-health impact of outdoor and traffic-related air pollution: a European assessment, Lancet N. Am. Ed. 356 (2000) 795–801.

[2] S.E. Nicholson, A pollution model for street-level air, Atmos. Environ. 9 (1975) (1967) 19–31.

[3] D.J. Nowak, D.E. Crane, J.C. Stevens, Air pollution removal by urban trees and shrubs in the United States, Urban For. Urban Green. 4 (2006) 115–123.

[4] S.M. Salim, R. Buccolieri, A. Chan, S.D. Sabatino, Numerical simulation of atmospheric pollutant dispersion in an urban street canyon: comparison between RANS and LES, J. Wind Eng. Ind. Aerodyn. 99 (2011) 103–113.

[5] B. Stathopoulos, CFD simulation of micro-scale pollutant dispersion in the built environment, Build. Environ. 64 (2013) 225–230.

[6] Y. Zhang, Z. Gu, C.W. Yu, Review on numerical simulation of airflow and pollutant dispersion in urban street canyons under natural background wind condition, Aerosol Air Qual. Res. 18 (2018) 780–789.

[7] C.H. Chang, R.N. Meroney, Concentration and flow distributions in urban street canyons: wind tunnel and computational data, J. Wind Eng. Ind. Aerodyn. 91 (2003) 1141–1154.

[8] R.W. Macdonald, R.F. Griffiths, D.J. Hall, A comparison of results from scaled field and wind tunnel modelling of dispersion in arrays of obstacles, Atmos. Environ. 32 (1998) 3845–3862.

[9] Z.L. Gu, Y.W. Zhang, Y. Cheng, S.C. Lee, Effect of uneven building layout on air flow and pollutant dispersion in non-uniform street canyons, Build. Environ. 46 (2011) 2657–2665.

[10] C. Liu, D. Leung, M. Barth, On the prediction of air and pollutant exchange rates in street canyons of different aspect ratios using large-eddy simulation, Atmos. Environ. 39 (2005) 1567–1574.

[11] S.J. Jeong, M.J. Andrews, Application of the k-ε turbulence model to the high Reynolds number skimming flow field of an urban street canyon, Atmos. Environ. 36 (2002) 1137–1145.

[12] M. Pavageau, M. Schatzmann, Wind tunnel measurements of concentration fluctuations in an urban street canyon, Atmos. Environ. 33 (1999) 3961–3971.

[13] P. Kastner-Klein, R. Berkowicz, R. Britter, The influence of street architecture on flow and dispersion in street canyons, Meteorol. Atmos. Phys. 87 (2004) 121–131.

[14] X. Xie, Z. Huang, J. Wang, X. Zheng, The impact of solar radiation and street layout on pollutant dispersion in street canyon, Build. Environ. 40 (2005) 201–212.

[15] J.J. Kim, J.J. Baik, A numerical study of the effects of ambient wind direction on flow and dispersion in urban street canyons using the RNG k-ε turbulence model, Atmos. Environ. 38 (2004) 3039–3048.

[16] L. Soulhac, R.J. Perkins, P. Salizzoni, Flow in a street canyon for any external wind direction, Bound. Layer Meteorol. 126 (2008) 365–388.

[17] J. Baker, H.L. Walker, X. Cai, A study of the dispersion and transport of reactive pollutants in and above street canyons—a large eddy simulation, Atmos. Environ. 38 (2004) 6883–6892.

[18] M. Moradpour, H. Afshin, B. Farhanieh, A numerical study of reactive pollutant dispersion in street canyons with green roofs, Build. Simul. 11 (2018) 125–138.

[19] T. Ming, C. Nie, W. Li, X. Kang, Y. Wu, M. Zhang, C. Peng, Numerical study of reactive pollutants diffusion in urban street canyons with a viaduct, Build. Simul. 15 (7) (2021) 1227–1241 pp. 1–15, Springer.

[20] Z. Ning, NOx and CO fluctuations in a busy street canyon, Environments 8 (12) (2021) 137–149.

[21] K. Uehara, S. Murakami, S. Oikawa, S. Wakamatsu, Wind tunnel experiments on how thermal stratification affects flow in and above urban street canyons, Atmos. Environ. 34 (2000) 1553–1562.

[22] C. Cai, T. Ming, W. Fang, R.D. Richter, C. Peng, The effect of turbulence induced by different kinds moving vehicles in street canyons, Sustain. Cities Soc. 54 (2020) 102015.

[23] Z. Li, T. Shi, Y. Wu, H. Zhang, N. Zhou, Effect of traffic tidal flow on pollutant dispersion in various street canyons and corresponding mitigation strategies, Energy Built Environ. 1 (2020) 242–253.

[24] T. Shi, T. Ming, Y. Wu, C. Peng, R.D. Richter, The effect of exhaust emissions from a group of moving vehicles on pollutant dispersion in the street canyons, Build. Environ. 181 (2020) 107–120.

[25] G. Duan, P. Brimblecombe, Y. Chu, K. Nagn, Turbulent flow and dispersion inside and around elevated walkways, Build. Environ. 173 (2020).

[26] M. Tallis, G. Taylor, D. Sinnett, P. Freer-Smith, Estimating the removal of atmospheric particulate pollution by the urban tree canopy of London, under current and future environments, Landsc. Urban Plan. 103 (2011) 129–138.

[27] J. Hang, Z. Xian, D. Wang, C.M. Mak, B. Wang, Y. Fan, The impacts of viaduct settings and street aspect ratios on personal intake fraction in three-dimensional urban-like geometries, Build. Environ. 143 (2018) 138–162.

[28] S. Ding, Y. Huang, P. Cui, J. Wu, M. Li, D. Liu, Impact of viaduct on flow reversion and pollutant dispersion in 2D urban street canyon with different roof shapes-Numerical simulation and wind tunnel experiment, Sci. Total 671 (2019) 976–991.

[29] J. Hang, Y. Li, R. Buccolieri, M. Sandberg, S. Di Sabatino, On the contribution of mean flow and turbulence to city breathability: the case of long streets with tall buildings, Sci. Total Environ. 416 (2012) 362–373.

[30] J. Hang, Q. Wang, X. Chen, M. Sandberg, W. Zhu, R. Buccolieri, S. Di Sabatino, City breathability in medium density urban-like geometries evaluated through the pollutant transport rate and the net escape velocity, Build. Environ. 94 (2015) 166–182.

[31] P. Lercher, Environmental noise and health: an integrated research perspective, Environ. Int. 22 (1996) 117–129.

[32] G. Licitra, L. Fredianelli, D. Petri, M.A. Vigotti, Annoyance evaluation due to overall railway noise and vibration in Pisa urban areas, Sci. Total Environ. 568 (2016) 1315–1325.

[33] K. Sygna, G.M. Aasvang, G. Aamodt, B. Oftedal, N.H. Krog, Road traffic noise, sleep and mental health, Environ. Res. 131 (2014) 17–24.

[34] P. Begou, P. Kassomenos, A. Kelessis, Effects of road traffic noise on the prevalence of cardiovascular diseases: the case of Thessaloniki, Greece, Sci. Total Environ. 703 (2020) 134477.

[35] N. Roswall, O. Raaschou-Nielsen, S.S. Jensen, A. Tjønneland, M. Sørensen, Long-term exposure to residential railway and road traffic noise and risk for diabetes in a Danish cohort, Environ. Res. 160 (2018) 292–297.

[36] A. Recio, C. Linares, J.R. Banegas, J. Díaz, Road traffic noise effects on cardiovascular, respiratory, and metabolic health: an integrative model of biological mechanisms, Environ. Res. 146 (2016) 359–370.

[37] E.S. Lee, D.R. Ranasinghe, F.E. Ahangar, S. Amini, S. Mara, W. Choi, S. Paulson, Y. Zhu, Field evaluation of vegetation and noise barriers for mitigation of near-freeway air pollution under variable wind conditions, Atmos. Environ. 175 (2018) 92–99.

[38] A. Pasquier, M. André, Considering criteria related to spatial variabilities for the assessment of air pollution from traffic, Transp. Res. Proced. 25 (2017) 3354–3369.

[39] N. Reiminger, X. Jurado, J. Vazquez, C. Wemmert, N. Blond, M. Dufresne, J. Wertel, Effects of wind speed and atmospheric stability on the air pollution reduction rate induced by noise barriers, J. Wind Eng. Ind. Aerodyn. 200 (2020) 104160.

[40] R. Baldauf, E. Thoma, A. Khlystov, V. Isakov, G. Bowker, T. Long, R. Snow, Impacts of noise barriers on near-road air quality, Atmos. Environ. 42 (2008) 7502–7507.

[41] L. Gong, X. Wang, Numerical study of noise barriers' side edge effects on pollutant dispersion near roadside under various thermal stability conditions, Fluids 3 (2018) 105.

[42] C. Hao, X. Xie, Y. Huang, Z. Huang, Study on influence of viaduct and noise barriers on the particulate matter dispersion in street canyons by CFD modeling, Atmos. Pollut. Res. 10 (2019) 1723–1735.

[43] H. Zhi, Z. Qiu, W. Wang, G. Wang, Y. Hao, Y. Liu, The influence of a viaduct on PM dispersion in a typical street: field experiment and numerical simulations, Atmos. Pollut. Res. 11 (2020) 815–824.

[44] A. Venkatram, V. Isakov, P. Des'Hmukh, R. Baldauf, Modeling the impact of solid noise barriers on near road air quality, Atmos. Environ. 141 (2016) 462–469.

[45] F.E. Ahangar, D. Heist, S. Perry, A. Venkatram, Reduction of air pollution levels downwind of a road with an upwind noise barrier, Atmos. Environ. 155 (2017) 1–10.

[46] R.W. Baldauf, V. Isakov, P. Deshmukh, A. Venkatram, B. Yang, K.M. Zhang, Influence of solid noise barriers on near-road and on-road air quality, Atmos. Environ. 129 (2016) 265–276.

[47] J. Hang, Z. Luo, X. Wang, L. He, B. Wang, W. Zhu, The influence of street layouts and viaduct settings on daily carbon monoxide exposure and intake fraction in idealized urban canyons, Environ. Pollut. 220 (2017) 72–86.

[48] B. Li, Z. Qiu, J. Zheng, Impacts of noise barriers on near-viaduct air quality in a city: a case study in Xi'an, Build. Environ. 196 (2021) 107751.

[49] S. Wang, X. Wang, Modeling and analysis of the effects of noise barrier shape and inflow conditions on highway automobiles emission dispersion, Fluids 4 (2019) 151.

[50] L. He, J. Hang, X. Wang, B. Lin, X. Li, G. Lan, Numerical investigations of flow and passive pollutant exposure in high-rise deep street canyons with various street aspect ratios and viaduct settings, Sci. Total Environ. 584 (2017) 189–206.

[51] K. Nazridoust, G. Ahmadi, Airflow and pollutant transport in street canyons, J. Wind Eng. Ind. Aerodyn. 94 (2006) 491–522.

[52] B. Blocken, T. Stathopoulos, P. Saathoff, X. Wang, Numerical evaluation of pollutant

dispersion in the built environment: comparisons between models and experiments, J. Wind Eng. Ind. Aerodyn. 96 (2008) 1817–1831.

[53] V.D. Assimakopoulos, H. ApSimon, N. Moussiopoulos, A numerical study of atmospheric pollutant dispersion in different two-dimensional street canyon configurations, Atmos. Environ. 37 (2003) 4037–4049.

[54] K.K. Leung, C.H. Liu, C.C. Wong, J.C. Lo, G.C. Ng, On the study of ventilation and pollutant removal over idealized two-dimensional urban street canyons, Build. Simul. 5 (4) (2012) 359–369 Springerpp.ˆ.

[55] S.T. Omaye, Metabolic modulation of carbon monoxide toxicity, Toxicology 180 (2002) 139–150.

[56] T. Ming, T. Shi, H. Han, S. Liu, Y. Wu, W. Li, C. Peng, Assessment of pollutant dispersion in urban street canyons based on field synergy theory, Atmos. Pollut. Res. 12 (2021) 341–356.

[57] T. Ming, H. Han, Z. Zhao, R. de Richter, Y. Wu, W. Li, N.H Wong, Field synergy analysis of pollutant dispersion in street canyons and its optimization by adding wind catchers, Build. Simul. 14 (2) (2021) 391–405 Springerpp.ˆ.

[58] X.X. Li, D.Y. Leung, C.H. Liu, K.M. Lam, Physical modeling of flow field inside urban street canyons, J. Appl. Meteorol. Climatol. 47 (2008) 2058–2067.

[59] R.N. Meroney, M. Pavageau, S. Rafailidis, M. Schatzmann, Study of line source characteristics for 2-D physical modelling of pollutant dispersion in street canyons, J. Wind Eng. Ind. Aerodyn. 62 (1996) 37–56.

[60] B. Blocken, T. Stathopoulos, J. Carmeliet, J.L. Hensen, Application of computational fluid dynamics in building performance simulation for the outdoor environment: an overview, J. Build. Perform. Simul. 4 (2011) 157–184.